Supporting Information

Decoupling High-Temperature Phase Transition and Charge-Transfer Emission in a Crown Ether-Based Crystal

Junchao Liu,[a]* Xinyi Yang,[a] Shuqi Han,[a] Wanying Zhang[b] and Pingping Shi[a]

[a] School of Chemical and Environmental Engineering, Anhui Polytechnic University, Wuhu 241000, China.
[b] School of Mathematics and Physics, Bengbu University, Bengbu 233030, China.

*Corresponding Author: Junchao Liu (liujunchao@ahpu.edu.cn.)

Experimental Procedures

Elemental analysis

The elemental compositions (C, H, N) of the samples were determined using an Elementar UNICUBE CHNS/O elemental analyzer. Sulfanilamide served as the reference standard for instrument calibration. For analysis, crystalline samples weighing 2–3 mg were sealed in tin, followed by high-temperature combustion at 1150 °C under a helium atmosphere with oxygen injection to achieve full oxidation. The resulting combustion gases were separated and detected by a thermal conductivity detector (TCD), enabling accurate determination of the elemental content of the samples. The results are as follows:
Compound **1** (2-F): Calculated for $C_{20}H_{35}F_7NO_6P$: C, 43.72%; H, 6.42%; N, 2.55%. Found: C, 43.57%; H, 6.74%; N, 2.47%.
Compound **2** (3-F): Calculated for $C_{20}H_{35}F_7NO_6P$: C, 43.72%; H, 6.42%; N, 2.55%. Found: C, 44.02%; H, 6.76%; N, 2.48%.
Compound **3** (4-F): Calculated for $C_{20}H_{35}F_7NO_6P$: C, 43.72%; H, 6.42%; N, 2.55%. Found: C, 44.02%; H, 6.46%; N, 2.43%.

NMR measurements

^{1}H NMR (500 MHz) spectra were recorded on Bruker Magnet System 500'54 Ascend. Chemical shifts for ^{1}H NMR spectra are reported as ppm relative to the residual proton signal of D_2O at 4.79 ppm (s). The results of NMR spectroscopy:
Compound **1**: ^{1}H NMR (500 MHz, D_2O) δ 7.31 (dd, J = 10.5, 4.8 Hz, 2H), 7.21 – 7.08 (m, 2H), 3.64 (s, 24H), 3.24 (t, J = 7.2 Hz, 2H), 3.01 (t, J = 7.2 Hz, 2H).
Compound **2**: ^{1}H NMR (500 MHz, D_2O) δ 7.37 (dd, J = 14.4, 7.2 Hz, 1H), 7.10 (d, J = 7.6 Hz, 1H), 7.05 (t, J = 9.1 Hz, 2H), 3.64 (s, 24H), 3.25 (t, J = 7.3 Hz, 2H), 2.98 (t, J = 7.2 Hz, 2H).
Compound **3**: ^{1}H NMR (500 MHz, D_2O) δ 7.34 – 7.23 (m, 2H), 7.10 (t, J = 8.8 Hz, 2H), 3.64 (s, 24H), 3.23 (t, J = 7.3 Hz, 2H), 2.95 (t, J = 7.2 Hz, 2H).

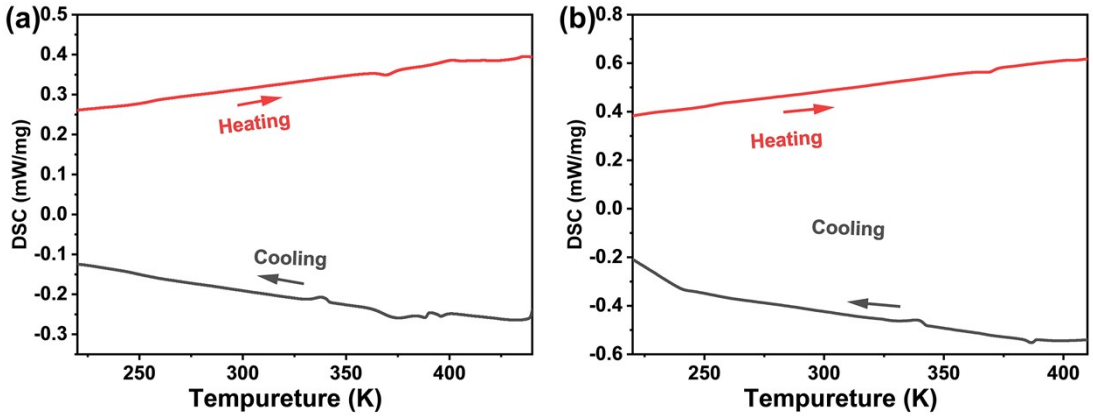

Fig. S1 DSC curves of compound **2** (a) and **3** (b) during heating and cooling cycles. Neither compound exhibits any obvious endothermic or exothermic peak in the measured temperature range, indicating the absence of a reversible solid–solid phase transition.

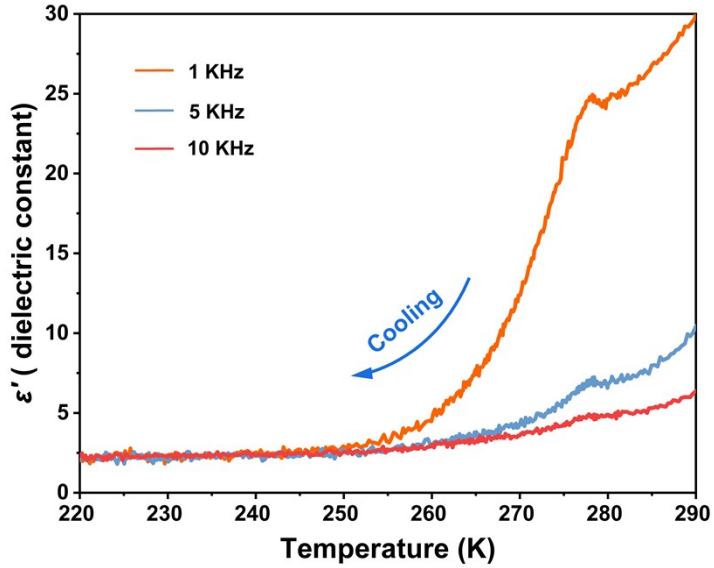

Fig. S2 Temperature-dependent real part of the dielectric constant of compound **1** measured at frequencies of 1 KHz, 5 KHz, and 10 KHz during cooling from 220 K to 290 K.

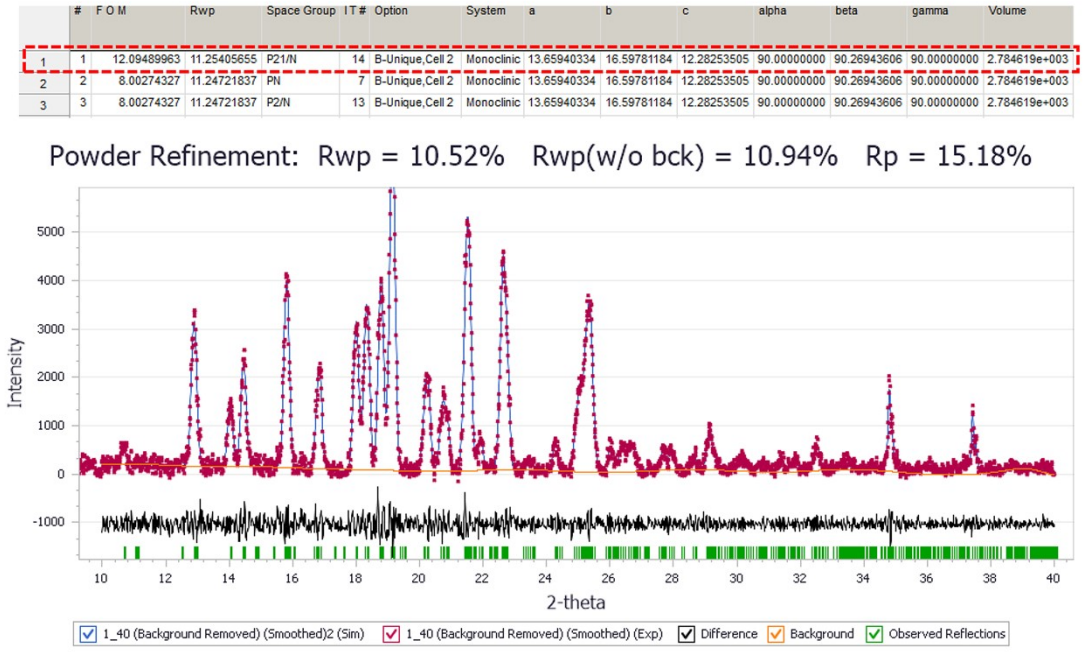

Fig. S3 Structural refinement results of powder X-ray diffraction data for **1** in the high-temperature phase (423 K).

The indexing of the PXRD pattern reveals a monoclinic lattice. Through Pawley refinement, we obtained the monoclinic point group 2/*m*, with the most probable space group being $P2_1/n$. The refined cell parameters are a = 13.659(4) Å, b = 16.597(8) Å, c = 12.282(5) Å, β = 90.269(4)°, and V = 2784.6(19) Å³. The refinement converged with R_{wp} = 10.52% and R_p = 15.18%, confirming the phase purity of the compound and the high accuracy of the simulation methods.

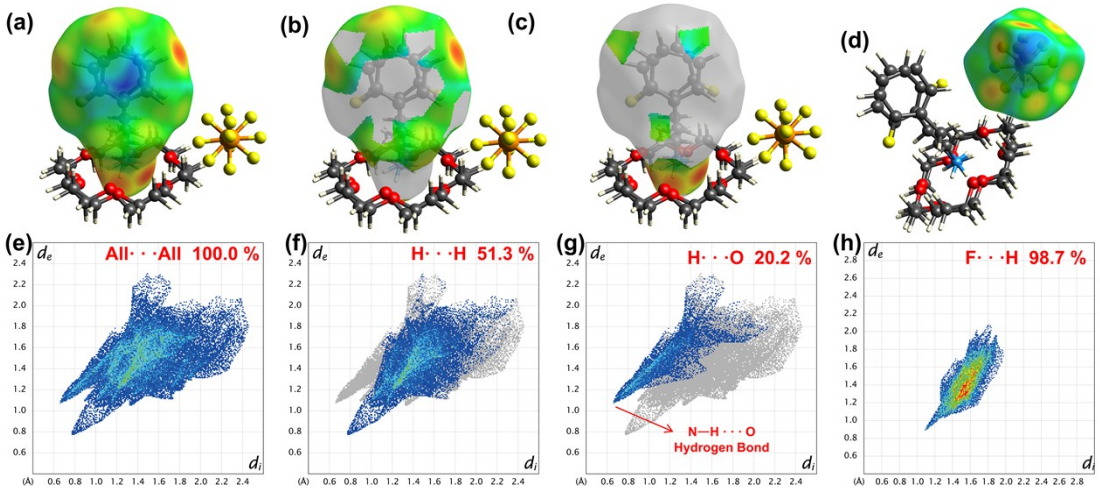

Fig. S4 Hirshfeld surfaces (d_i) and two-dimensional (2D) fingerprint plots of compound **1** at 298 K.

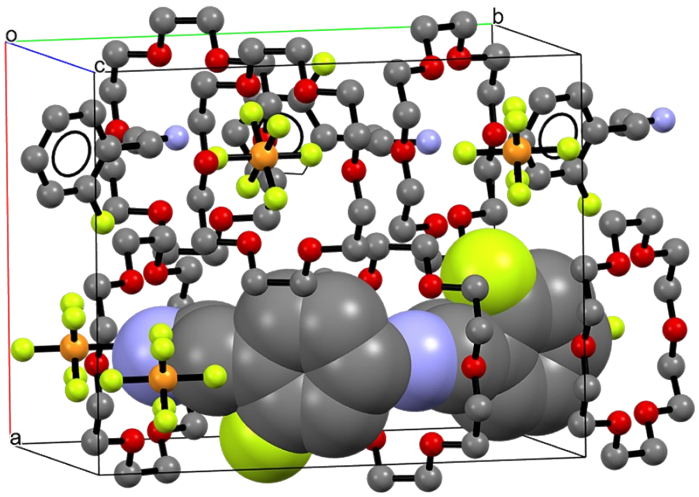

Fig. S5 Packing arrangement of 2-fluorophenethylammonium cations in the crystal lattice of compound **1**, where 18-crown-6 macrocycles act as spatial barriers to prevent close π-π stacking.

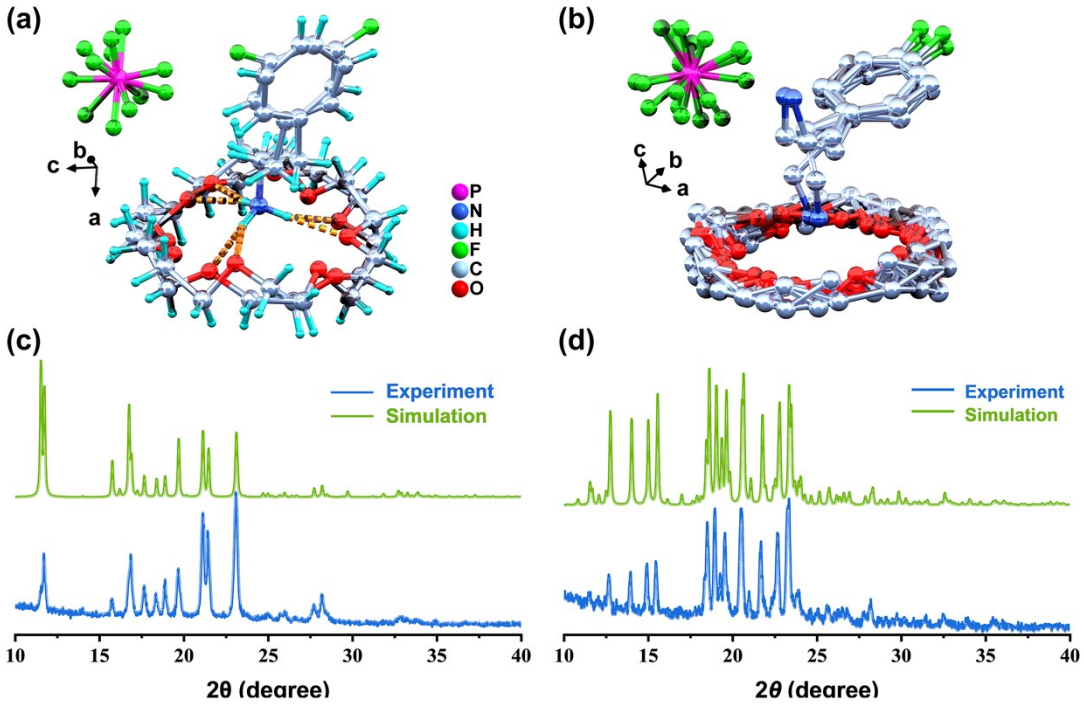

Fig. S6 Crystal structures of compounds **2** (a) and **3** (c) at 298 K. Powder X-ray diffraction patterns of compounds **2** (b) and **3** (d) at 298 K.

The crystal structures of the regioisomeric analogues with fluorine at the 3-position (compound **2**) and 4-position (compound **3**) were determined at 298 K. Both compounds adopt similar host–guest architectures as compound **1**, with the fluorophenethylammonium cation confined within the 18-crown-6 cavity through N–

H···O hydrogen bonds. Notably, distinct disorder behaviors are observed. In compound **2**, the 18-crown-6 ring, the PF_6^- anion, and the 3-fluorophenethylammonium cation all exhibit crystallographic disorder. In compound **3**, a more pronounced disorder is present at 298 K: the 18-crown-6 macrocycle, the PF_6^- anion, and the 4-fluorophenethylammonium cation are in a fourfold crystallographic disorder state, and the structure also possesses mirror symmetry along both the a and c axes. These disorder features contrast sharply with the structure of compound **1** at the same temperature, consistent with the absence of phase transitions in compounds **2** and **3**. Powder X-ray diffraction (PXRD) patterns measured at 298 K for both compounds show excellent agreement with the simulated patterns derived from single-crystal data, confirming the phase purity of the samples and the representativeness of the crystal structures.

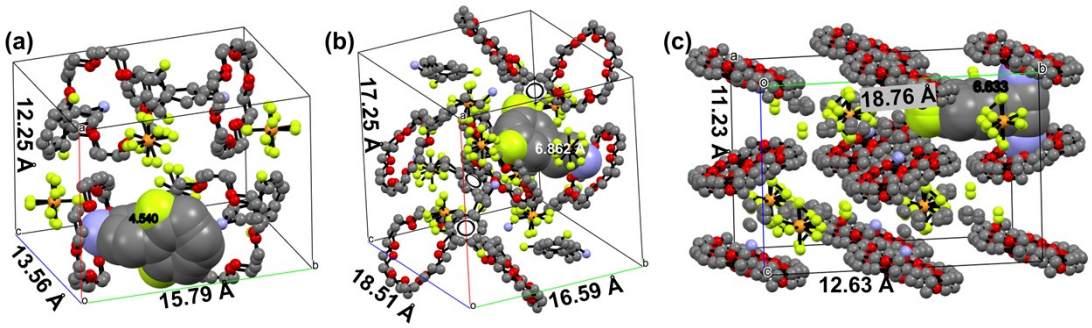

Fig. S7 Crystal packing of the cations in (a) compound **1** (2-fluoro), (b) compound **2** (3-fluoro), and (c) compound **3** (4-fluoro). The F···N distances are 4.540 Å, 6.862 Å, and 6.633 Å, respectively, showing the distinctly shorter intramolecular contact in the ortho isomer.

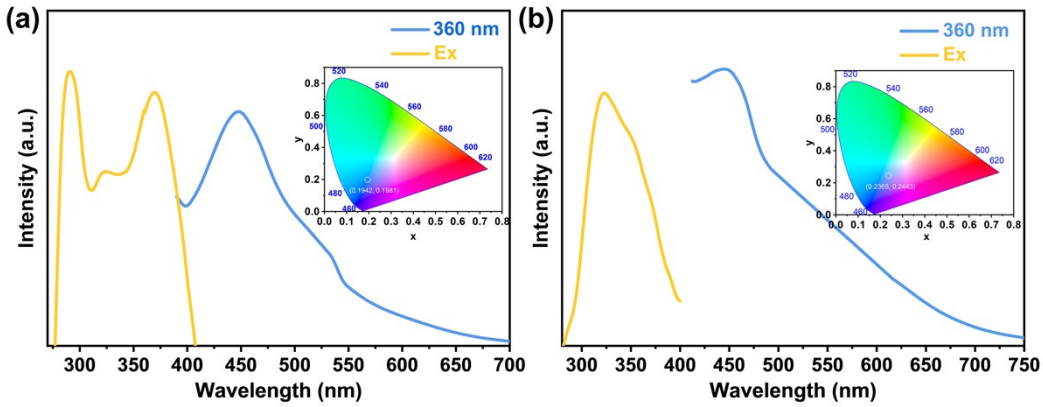

Fig. S8 Fluorescence spectra of compound **2** (a) and **3** (b) measured at room temperature. For each compound, the excitation spectrum (monitored at the emission maximum) and the emission spectrum (excited at 360 nm) are shown. Both compounds exhibit blue emission similar to compound **1**, indicating that supramolecular confinement activates luminescence regardless of the fluorine substitution position.

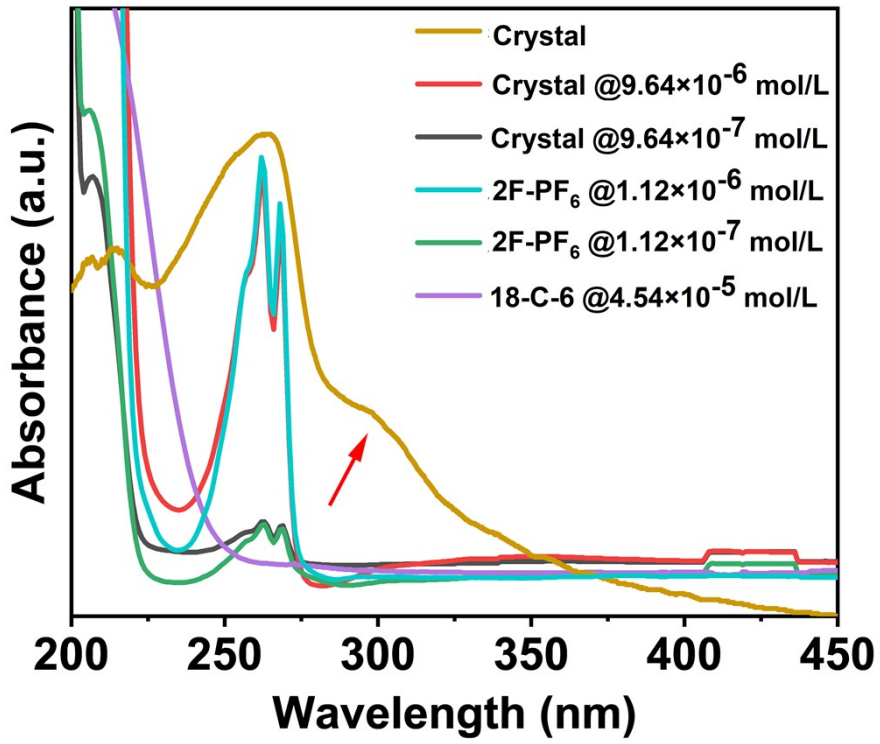

Fig. S9 UV-Vis absorption spectra of crystalline compound 1 (Cyrstal), compound **1** in methanol at different concentrations (Crystal@9.64×10^{-7} mol/L, Crystal@9.64×10^{-7} mol/L), 18-crown-6 in methanol (18-C-6), and 2-fluorophenethylammonium hexafluorophosphate in methanol (2F-PF_6).

The results show that in dilute methanol solution, the absorption spectrum of compound **1** is almost identical to that of the free 2-fluorophenethylammonium salt, displaying a maximum at 262 nm with a shoulder at 268 nm, indicating that the solution-phase UV absorption originates from the π→π* transition of the benzene ring.

Free 18-crown-6 at a concentration of 4.54×10^{-5} mol/L in methanol shows negligible absorption in the 200-800 nm range. In striking contrast, the crystalline solid of compound **1** exhibits a markedly different spectrum: in addition to a wide absorption at 266 nm, a new absorption band appears at approximately 300 nm, which suggests that the low-energy transition is a charge-transfer band. Notably, none of the solution samples show any detectable absorption in the 300 nm region. Consequently, the 300 nm band is unique to the crystalline state and disappears when the host–guest complex dissociates in dilute solution or when the individual components are measured separately.

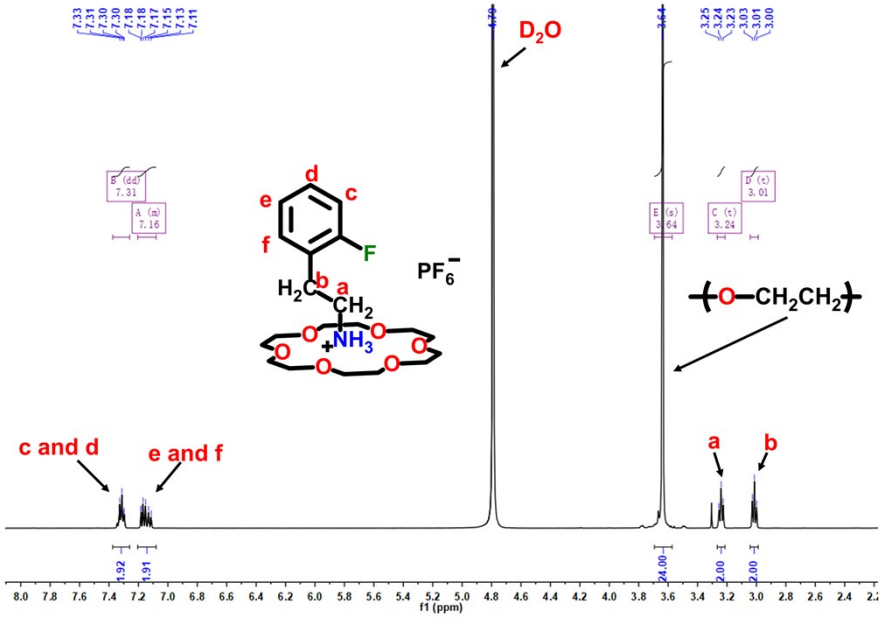

Fig. S10 ^{1}H NMR spectrum of compound **1** (500 MHz, D_2O).

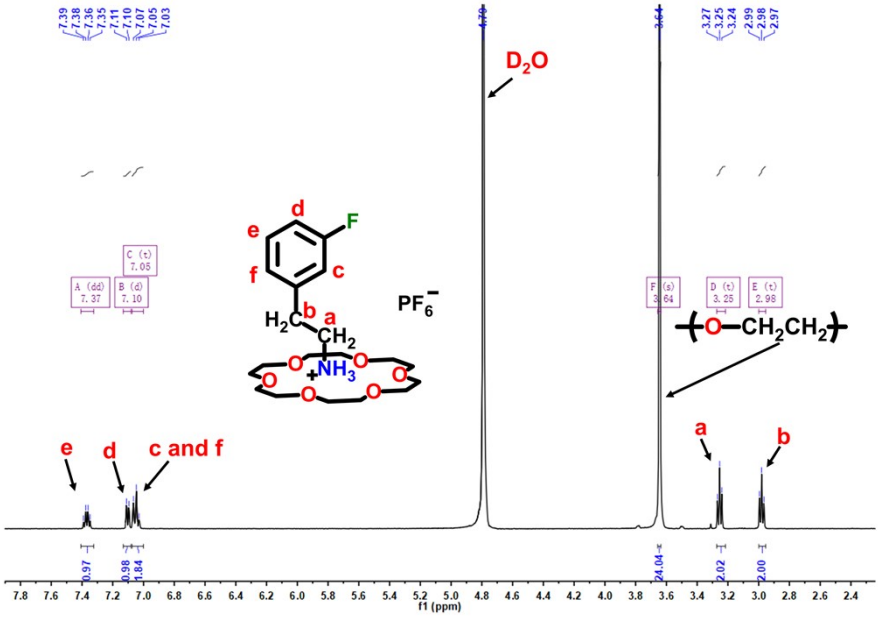

Fig. S11 ^{1}H NMR spectrum of compound **2** (500 MHz, D_2O).

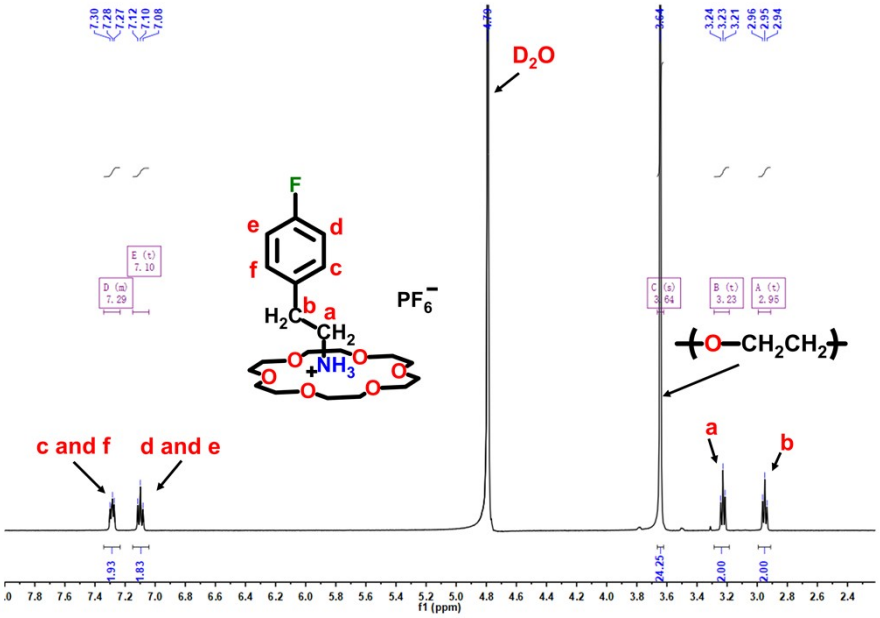

Fig. S12 ^{1}H NMR spectrum of compound **3** (500 MHz, D_2O).

Table S1. The crystal data and structure refinement for compounds **1, 2,** and **3.**

Compound	**1**		**2**	**3**
Empirical formula	$C_{20}H_{35}F_7NO_6P$		$C_{20}H_{35}F_7NO_6P$	$C_{20}H_{35}F_7NO_6P$
Formula weight	549.46		549.46	549.46
Temperature/K	298	173	298	298
Crystal system	Monoclinic	Monoclinic	Orthorhombic	Orthorhombic
Space group	$P2_1/n$	$P2_1/n$	*Pbca*	*Cmcm*
a (Å)	12.249(4)	12.3530(11)	17.2491(4)	11.231(4)
b (Å)	15.792(6)	15.1662(17)	16.5906(4)	18.764(6)
c (Å)	13.564(5)	13.4368(15)	18.5124(4)	12.639(4)
α (°)	90	90	90	90
β (°)	93.780(13)	92.638(10)	90	90
γ (°)	90	90	90	90
Volume ($Å^3$)	2618.3(16)	2514.7(5)	5297.7(2)	2663.5(15)
Z	4	4	8	4
$R_1[I \geq 2\sigma(I)]$	0.1476	0.1369	0.1529	0.1421
$wR_2[I \geq 2\sigma(I)]$	0.2389	0.2930	0.2346	0.1877
GOF	1.012	1.062	0.981	0.988
CCDC number	2527441	2527440	2545079	2545078

Note: The relatively high *R* values for all structures arise mainly from the inherent crystallographic disorder present in the materials. The crystal of compound **3** exhibits severe fourfold crystallographic disorder of both the 18-crown-6 macrocycle and the 4-fluorophenethylammonium cation at 298 K. As a result, the crystal habit description (_exptl_crystal_description) could not be reliably determined, and the data-to-parameter ratio is lower than ideal (PLAT088). Nevertheless, the structural model is well refined and the phase purity is confirmed by PXRD (Fig. S6).

Table S2. Hydrogen-bond parameters for compound **1** at 173 K and 298 K

Temperature	D–H···A	D–H (Å)	H···A (Å)	D···A (Å)	D–H···A (°)
298 K	N1-H1AC···O3	0.89	2.06	2.86(5)	149
	N1-H1AC···O4	0.89	2.43	2.82(3)	107
	N1-H1AD···O5	0.89	2.08	2.94(4)	162
	N1-H1AD···O6	0.89	2.31	2.84(3)	118
	N1-H1AE···O1	0.89	1,96	2.83(2)	165
	N1-H1AE···O2	0.89	2.33	2.72(4)	107
173 K	N1-H1A···O1	0.91	2.05	2.842(8)	145.1
	N1-H1B···O3	0.91	1.93	2.832(9)	168.6
	N1-H1C···O5	0.91	1.96	2.857(8)	168.3